Aquat Sci (2017) 79:995–1007
DOI 10.1007/s00027-017-0550-3

Aquatic Sciences

RESEARCH ARTICLE

High rates and close diel coupling of primary production and ecosystem respiration in small, oligotrophic lakes

Kenneth Thorø Martinsen[1] · **Mikkel René Andersen**[1] · **Theis Kragh**[1] · **Kaj Sand-Jensen**[1]

Received: 9 December 2016 / Accepted: 28 June 2017 / Published online: 5 July 2017

Abstract Studies on small, shallow lakes are few and have traditionally focused on humic lakes, whereas transparent, oligotrophic lakes dominated by submerged macrophytes have been overlooked. This may have given rise to a skewed perception of shallow lakes as being well mixed, turbid and dominated by ecosystem respiration relative to primary production. Mixing patterns and ecosystem metabolism in five oligotrophic shallow lakes dominated by charophytes were investigated in order to determine gross primary production, ecosystem respiration, their regulation and mutual coupling in this very common lake type. Although lakes were very shallow (<0.5 m), high charophyte biomass caused strong daytime stratification followed by nocturnal mixing. Despite the nutrient-poor water, volumetric rates of production and respiration during spring–summer were high compared to most medium to large lakes. This intensive metabolism is likely a result of the high charophyte biomass and the shallow mixed surface layer. Areal rates of production and respiration were also high compared to values from other aquatic systems. Strong coupling between daily rates of production and respiration suggested that the majority of organic substrates for ecosystem respiration were produced within the lakes. Net ecosystem production was slightly positive during the growth season. This study highlights the role of submerged macrophytes as primary drivers of temperature dynamics, stratification-mixing as well as high metabolism in small, shallow lakes with dense vegetation.

Keywords Small lake · Ecosystem metabolism · Charophytes · Oligotrophic

Introduction

The realization that small lakes (<1 ha) are the most abundant water bodies globally (Downing et al. 2006; Verpoorter et al. 2014), and that their role in global carbon budgets has been grossly underestimated (Holgerson and Raymond 2016) ought to stimulate research of lakes in this size range (Downing 2010). Traditionally, medium-sized- and large lakes have been the prominent research object. This study reports results from an investigation of ecosystem metabolism in five small, shallow, calcareous lakes dominated by charophytes (*Chara* spp.) on the nutrient-poor alvar plains of Öland, Sweden in order to broaden the knowledge of shallow oligotrophic lakes' metabolism and ecology.

A recent study on a small alvar lake showed that dense charophyte stands and relatively high rates of GPP and R gradually developed during spring and early summer despite oligotrophic conditions and extremely low concentrations of ammonium, nitrate and phosphate in the water (Christensen et al. 2013). The main nutrient source for the dense charophyte stands is the sediment. Nutrients are absorbed by rhizoids and transported upward to apical meristems of the charophytes by cytoplasmic streaming (Vermeer et al. 2003). Nocturnal convective mixing of the shallow water column after daytime vertical stratification also re-distributes dissolved nutrients and inorganic carbon in

Electronic supplementary material The online version of this article (doi:10.1007/s00027-017-0550-3) contains supplementary material, which is available to authorized users.

✉ Kenneth Thorø Martinsen
kenneth2810@gmail.com

[1] Freshwater Biological Laboratory, Biological Institute, University of Copenhagen, Universitetsparken 4, 3rd. floor, 2100 Copenhagen, Denmark

the water column. Nutrients and inorganic carbon released by decomposition and mineralization processes in the sediments are distributed to the entire water column each night and can stimulate new charophyte production (Andersen et al. 2016).

Dense charophyte stands approach the water surface and strongly attenuate incident irradiance, and consequently phytoplankton and benthic microalgae photosynthesis is effectively constrained (Andersen et al. 2016). For this reason, charophytes were responsible for almost the entire primary production and about 90% of community respiration in a small charophyte dominated alvar lake (Andersen 2015). In dense charophyte stands with high internal self-shading, primary production is probably high because almost all of the available light is absorbed by photosynthetic pigments (Binzer et al. 2006). Macrophyte stands can reach comparable high levels of areal primary production as in very dense phytoplankton communities (Krause-Jensen and Sand-Jensen 1998).

The terrestrial soil covering the limestone alvar plains is very thin (typically 0–10 cm) and the vegetation cover is sparse (Sand-Jensen et al. 2015). External input of nutrients and organic matter to the charophyte lakes is especially low during late spring and summer when evapotranspiration exceeds precipitation, and surface water flow to the lakes is negligible (Christensen et al. 2013). Labile organic matter for respiration mainly derives from autochthonous production within the lakes, and it is processed faster than terrestrially derived allochthonous organic matter (Del Giorgio et al. 1999).

Recent studies of oligotrophic lakes and streams confirm that organic substrates from intra-system primary production are rapidly consumed by respiration of autotrophs themselves along with closely coupled bacteria. Thus, on an overall basis, respiration rates are constrained by the availability of organic substrates (Alnoee et al. 2015; Richardson et al. 2016; Solomon et al. 2013). If close coupling between autochthonous production and heterotrophic consumption of organic matter is a general feature of oligotrophic, charophyte-rich lakes then gross primary production (GPP) and ecosystem respiration (R) could be similar in magnitude and closely coupled in time. Linear regression analysis of daily GPP and R should then follow a linear relationship with a slope (β) close to 1.0 and a background respiration (R_{base}) close to zero according to $R = \beta GPP + R_{base}$ (Solomon et al. 2013).

Our objective was to quantify daily rates of GPP and R in five small charophyte-rich lakes on Öland's alvar during spring and early summer of 2015 and 2016. Four specific hypotheses were tested: (1) ecosystem rates of GPP and R exhibit approximately similar rates, (2) GPP and R are closely coupled in time resulting in close to 1:1 linear relationships between daily rates, (3) background respiration (R_{base}) is low because respiration is limited by organic production within the lake, and, in comparison with other aquatic ecosystems (Hoellein et al. 2013), (4) areal and volumetric rates of GPP and R in the shallow, oligotrophic charophyte lakes can be relatively high.

Materials and methods

Site description

The investigated small lakes are located on Räpplinge Alvar, Öland, Sweden (56.8113°N 16.6085°E, Fig. 1). They receive water predominantly from precipitation and surface runoff and undergo large fluctuations in water level. During winter, heavy precipitation and low evapotranspiration may cause otherwise separated lakes to merge and deliver water by overflow to other lakes and intermittent streams. During summer, the shallowest lakes ($z_{max} = 0.2$ m) often dry out and support only a small biomass of submerged macrophytes. The deeper lakes ($z_{max} = 0.5$ m), which rarely dry out entirely, have thin sediments (5–10 cm) deposited on the hard rock surface and support high biomasses of submerged charophytes across most of the bottom. Lake water is transparent, alkaline and very low in nutrients (Christensen et al. 2013).

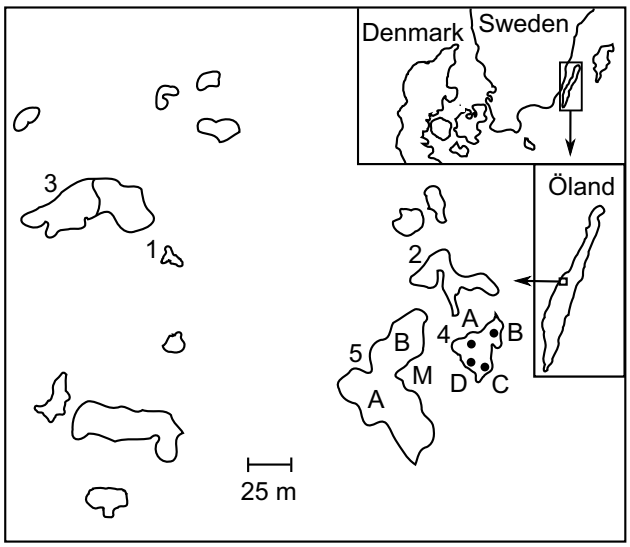

Fig. 1 Map showing southern Scandinavia, the location of Öland, Räpplinge Alvar and the five studied lakes and individual sites. The meteorological station (*M*) is marked

Data collection

Data on weather, basic lake parameters as well as continuous measurements of temperature and dissolved oxygen for estimation of lake metabolism were collected in five different lakes from late March to early June 2015 and again from late May to mid-June 2016 (Table 1). Meteorological data were measured next to the lakes within a distance of 10–200 m. Sensors were placed 2 m above the ground to measure incident irradiance (PAR, HOBO S-LIA-M003, Onset Computers, Bourne, Ma, USA), wind speed and direction (HOBO S-WSET-A, Onset Computers), air temperature and relative humidity (HOBO U23 Pro v2, Onset Computers) as well as barometric pressure (HOBO U-20-001-04, Onset Computers). Data were measured and logged every 10 min (Hobo microstation, H21-002, Onset Computers). Daily data on precipitation were obtained from an official weather station (Skedemosse) located only 10 km from the study site (SMHI).

Lake bathymetry was determined by measuring water depth (accuracy 0.5 cm) for every 0.5 m along at least two transects across the surface of each lake. Height and percent cover of the charophyte canopy were determined simultaneously with measurements of water depth. Underwater sensors in each lake measured pressure (HOBO U-20-001-04, Onset Computers); by using reference barometric pressure recorded at the weather station, water depth was calculated for every day (HOBOware, Onset Computers) with an accuracy of 3 mm, allowing daily calculations of lake area and water volume.

Dissolved oxygen was measured using MiniDot optode sensors (PME, Vista, CA, USA). Sensors were calibrated before and after deployment; no sensor drift was observed. In lakes with dense stands of submerged macrophytes and maximum water depth above 20 cm, two oxygen sensors and several temperature sensors (3–6, HOBO UA-002-64, Onset Computers, accuracy of 0.53 °C) were mounted on vertical steel pegs rising from heavy steel plates buried in the sediment. Temperature sensors were mounted with distances of 5–10 cm. One oxygen sensor was placed in the free water overlying the charophyte canopy, the other sensor was placed within the canopy 5–10 cm above the sediment. Temperature sensors also recorded light intensity (lux). These values were used to estimate the proportion of surface light passing the charophyte canopy to the sediment surface. In shallow lakes and in shallow sections of deeper lakes with water depths less than 20 cm, one oxygen sensor was placed in the middle of the water column. Sensors recorded the values every 10 min.

Acid neutralizing capacity (ANC = alkalinity) of water samples was measured by acidimetric titration (Gran 1952) and dissolved inorganic carbon (DIC) was calculated from pH and alkalinity (Lewis and Wallace 1998). Nutrients were determined by standard methods on an autoanalyzer (AA3 HR AutoAnalyzer, SEAL, USA).

During June 2016, charophyte biomass was measured in all four studied lakes by sampling charophytes at five random sites with a plastic cylinder (10 cm in inner diameter). Lake 4 was sampled both in 2015 and 2016. The material was rinsed, dried at 105 °C and weighed.

Estimating ecosystem metabolism

Diel ecosystem metabolism was estimated using measurements of oxygen and temperature recorded from the surface oxygen sonde overlying the charophyte canopy along with supporting data. Small gaps in data series (<1 h), except for dissolved oxygen, were filled by linear interpolation; days with gaps in oxygen data were excluded from further analysis. A few lake days with heavy rain (>5 mm per event) were excluded from further analysis (i.e., 29–30 March, 1 and 5 May 2015) because noise was too high. Moreover, 1 day was excluded when sensors were maintained and calibrated (14 May 2015). The analyzed lakes and periods are shown in Table 1.

Changes in dissolved oxygen can be attributed to GPP, R and atmospheric gas flux (F) according to the equation (Odum 1956):

$$\frac{\Delta O_2}{\Delta t} = GPP - R + F. \quad (1)$$

Equation 1 can be modified to

$$Y_{t+1} = Y_t + GPP_t - R_t + F_t + Z_t, \quad (2)$$

in which Z is an error term and the time step (t) is 10 min. GPP and R can be described using several relationships (Hanson et al. 2008). According to a previous study in one of the small lakes (Christensen et al. 2013), the best fitting relationships described GPP as a hyperbolic function of irradiance (Jassby and Platt 1976) and R as a function of temperature by the Arrhenius equation (Jørgensen and Bendoricchio 2001):

$$GPP = P_{\max} \tanh\left(\alpha \frac{PAR}{P_{\max}}\right), \quad (3)$$

$$R = R_{\max}\, \theta^{(T-20)}. \quad (4)$$

Maximum GPP (P_{max}, g O_2 m^{-3} Δt^{-1}) is GPP at light saturation, and α [g O_2 m^{-3} Δt^{-1} (μmol m^{-2} s^{-1})$^{-1}$] is the photosynthetic efficiency at limiting irradiance. R_{max} (g O_2 m^{-3} Δt^{-1}) is maximum respiration at a reference temperature (20 °C) and θ is a constant accounting for the influence of temperature on R. We applied a standard value for θ of 1.073 °C^{-1}, which is equivalent to a Q_{10} of 2.0 (Jørgensen and Bendoricchio 2001). Direct

Table 1 Five charophyte lakes examined on Öland in March–June 2015 and June 2016

Lake	Site	Period	Surface area (m^2)	z_{site} (cm)	z_{mean} (cm)	Alkalinity (meq L^{-1})	Biomass (g DW m^{-2})	Cover (%)	Height (cm)	$Light_{bottom}$ (%)	NO_3^- (µg L^{-1})	NH_4^+ (µg L^{-1})	PO_4^{3-} (µg L^{-1})
1		June 2015	81	31 (30–33)	22	1.3				0.1			
3		June 2015	340	9 (7–11)	5	2.1						14[1]	3.2[a]
4	A	March–June 2015	855 (701–997)	46 (34–62)	25	1.1 (0.8–1.5)	796 (364–1023)			0.3		31[1]	2.3[a]
	B	March–June 2015		46 (34–62)									
	C	March–June 2015		17 (6–33)									
	D	May 2015		44 (32–60)									
5	A	March–June 2015	2158 (1610–3056)	52 (47–66)	17	1.0				0.2			
	B	June 2015		10 (7–12)									
1		June 2016	85	38 (34–43)	30	2.1 (1.2–2.6)	813 (589–1025)	97	23	0.03			
2		June 2016	311	25 (21–29)	17	1.2 (0.8–1.8)	319 (209–398)	89	9.6	0.1			
3		June 2016	431	17 (16–18)	12	1.8 (1.0-2.3)	327 (267–393)	76	5.1				
4	A	June 2016	827	43 (38–49)	31	1.0 (0.7–1.4)	775 (591–990)	92	23		9.4 ± 5.1	22 ± 7.3	1.7 ± 2.4

Characteristics are: surface area-water depth-alkalinity and characteristics of the charophyte vegetation (biomass, areal cover and canopy height). Mean depth (z_{mean}) and depth at measuring site (z_{site}) are provided. Presented are mean values with ranges in parenthesis. Inorganic nutrients in Lake 3 (2016) are provided as mean ± SD of 35, 20 and 35 samples for NO_3^-, NH_4^+ and PO_4^{3-}, respectively

[a]Measurements from summer 2009

measurements of temperature dependence of charophyte respiration were close to this selected value (Kragh et al. 2017).

Atmospheric gas exchange, F (g O_2 m^{-3} Δt^{-1}), was calculated as in Solomon et al. (2013)

$$F = -k\,(O_2 - O_{2sat})/z_{mix}, \quad (5)$$

in which k (m h^{-1}) is the gas transfer velocity, O_{2sat} is the oxygen saturation concentration for a given temperature (Weiss 1970) and z_{mix} is the thermocline depth calculated using rLakeAnalyzer (Read et al. 2011). Mixed layer depth was only calculated for sites with high density of submerged macrophytes and water depths greater than 0.2 m, while shallower sites with sparse plant cover were assumed to be fully mixed to the sediment surface. This assumption was tested and no difference was found between surface and bottom waters in a shallow section of Lake 4 (data not shown). The normalized gas transfer velocity (k_{600}, m h^{-1}), with k normalized to a Schmidt number of 600 (CO_2 at 20 °C), was calculated using an empirical relationship determined by direct gas flux measurements in Lake 4 as a function of wind speed (m s^{-1}) and wind gust speed (m s^{-1}) averaged for two hours prior to calculation (Andersen 2015):

$$wind\ speed < 2\ (m\ s^{-1});\ k_{600} = (0.14\ \cdot gust + 0.04)/100, \quad (6)$$

$$wind\ speed > 2\ (m\ s^{-1});\ k_{600} = (0.87\ \cdot gust - 2.10)/100.$$

Schmidt number (Sc) for oxygen was calculated as a function of temperature (Wanninkhof 1992). The gas transfer velocity (k) was calculated at ambient temperature from the ratio of Schmidt numbers (Jähne et al. 1987):

$$k = k_{600}\left(\frac{Sc}{600}\right)^{-0.5}. \quad (7)$$

The free parameters P_{max}, R_{max} and α (Eqs. 3, 4) were estimated for each lake-day by minimizing the negative log likelihood of the error term Z (Eq. 2, Hilborn and Mangel 1997). The Broyden–Fletcher–Goldfarb–Shanno optimization algorithm with the optim function in R (R Core Team 2016) was used with the free parameters forced to be positive. Each lake-day started at sunrise and lasted until sunrise the next day with night defined as the time when incident irradiance was zero. Volumetric rates (g O_2 m^{-3} day^{-1}) of GPP, R and NEP (NEP = GPP-R) were converted to rates per surface area (g O_2 m^{-2} day^{-1}) by multiplying with mean water depth, which was calculated from hypsographic measurements and lake water level. Metabolic rates per water volume used in the regression analysis between GPP and R were both normalized to 20 °C (GPP_{20} and R_{20}) by implementing the Arrhenius equation (Eq. 4) with the same temperature coefficient and daily mean water temperature.

The R-GPP relationship was analyzed by standardized major axis regression (model II regression; lmodel2 package in R). Respiration rates are shown as negative values to facilitate interpretation. The relationship between daily GPP and daily incident irradiance were fitted by using the nls function in R.

Quantifying uncertainty: the bootstrap analysis

A bootstrap procedure allowed estimation of uncertainty around daily estimates of the free parameters (Solomon et al. 2013; Van de Bogert et al. 2007). Here, residual bootstrapping was used to generate new diel oxygen curves. The initial estimation of the free parameters applying the above approach yields a model (DO_{mod}) of the diel oxygen signal (Eqs. 2–7). The residuals (res) are the difference between the measured diel oxygen curve (DO_{obs}) and modeled curve (DO_{mod}):

$$res = DO_{obs} - DO_{mod}. \quad (8)$$

The residuals are auto-correlated and can be described by a first-order auto-regressive scheme

$$res_{t+1} = \varphi\ res_t + \varepsilon, \quad (9)$$

in which ϕ is the auto-correlation coefficient and ε are residuals (white noise). Both terms are estimated for each lake day. Bootstrap datasets are generated by sampling with replacement from ε followed by recursion into the auto-regression scheme (Eq. 9) thus creating a new series of bootstrap residuals (res_{boot}) with the original auto-correlation structure, which can be added to DO_{mod} (Eq. 8, Politis 2003). By repeating this process many times (999) for each lake day, 95% confidence intervals can be estimated for each of the free parameters (Figure S1, Efron and Tibshirani 1993).

Results

Physical and chemical parameters

In the shallow water (<0.2 m) of Lake 4 loc. C, Lake 5 loc. B as well as Lake 3, the water columns were permanently mixed. Meanwhile, the other locations with deeper water (>0.2 m) in Lake 1, 2, 4 and 5 were stratified during daytime and mixed during nighttime. This recurring feature is pronounced during summer 2016 (Fig. 2). Exceptions to this pattern occurred during cold days with heavy rain or very low irradiance in which the water column remained mixed. In the morning, the water columns deeper than 0.2 m stratified as incident irradiance increased. Simultaneously, bottom waters within the canopy rapidly became hypoxic or anoxic, while surface

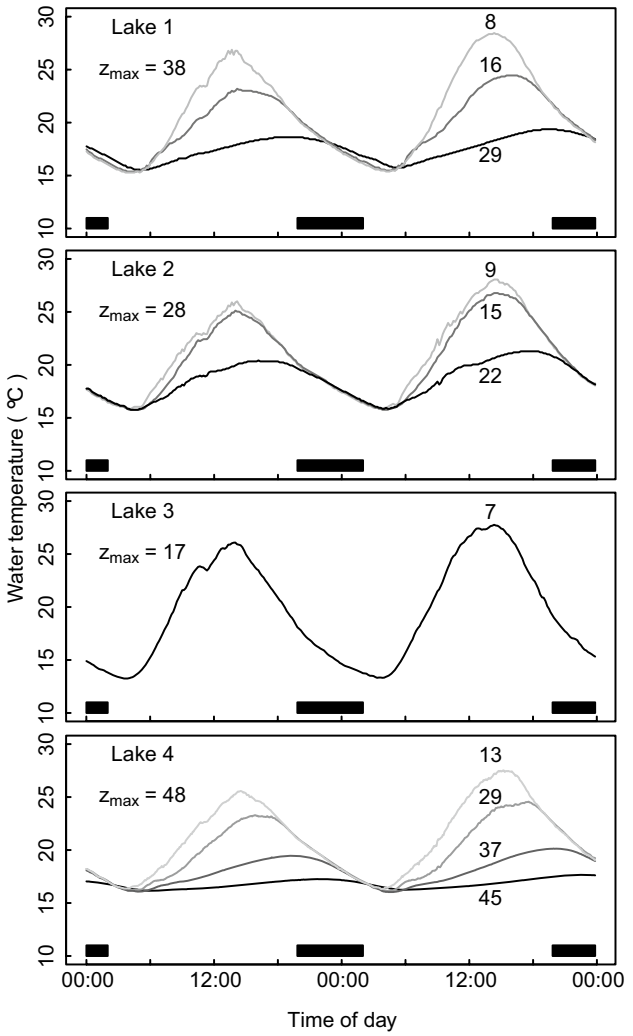

Fig. 2 Diel changes of temperature at different water depths in four charophyte lakes for 31 May and 1 June 2016. *Black bars* indicate night time. Depths of sensors and maximum depth are denoted (cm)

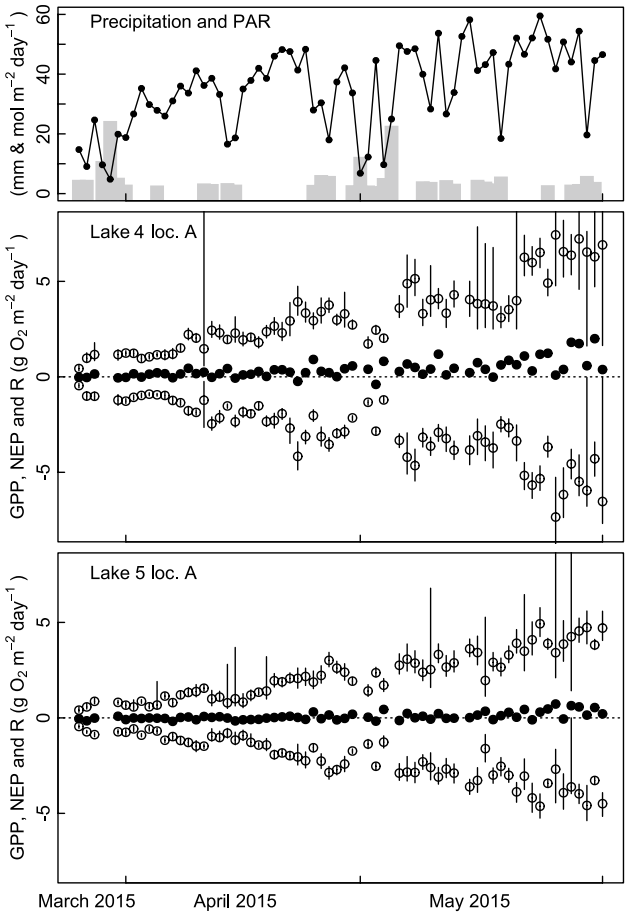

Fig. 3 Precipitation (mm), surface irradiance (mol photon m^{-2} day^{-1}) and areal rates of metabolism (g O_2 m^{-2} day^{-1}) in Lake 4 loc A and Lake 5 loc A during spring 2015. Daily GPP and R rates (*open circles*) with 95% CI and NEP (*filled circles*) are shown

waters became oxygen supersaturated (200–250% saturation). This vertical oxygen distribution reflects intense respiration in bottom waters and intense photosynthesis in surface waters (data not shown).

From late March to early June 2015, surface irradiance and water temperature in Lake 4 and 5 increased along with the diel amplitudes of temperature and oxygen (Figure S3). Fluctuating water levels followed the patterns of precipitation. During June 2016, precipitation was low and surface irradiance high, which promoted charophyte metabolism. Charophyte biomass was dense in all lakes, but significantly denser in the deeper Lakes 1 and 4 than in the shallower Lakes 2 and 3 (Table 1). Light only reached the sediment surface in locations with very shallow water and low charophyte biomass and cover (Lake 3, Lake 4 loc. C and Lake 5 loc. B; Table 1). At all other sites, the charophyte stands were dense and virtually no light (0–0.3% of surface irradiance) reached the sediment surface (Table 1).

Ecosystem metabolism

From 26 March to 1 June in 2015, GPP and R (g O_2 m^{-2} day^{-1}) increased about tenfold in Lakes 4 and 5. This development reflects the rise in irradiance, temperature and perhaps charophyte biomass (Fig. 3 and S3). GPP and R followed an approximately parallel course and were of similar magnitude. Rates of GPP and R relative to surface area were higher in Lake 4 than Lake 5. GPP in the two lakes was closely correlated over time ($r_s = 0.86$, $p < 0.001$, Spearman-rank), which probably reflects a common response to gradually increasing temperatures and incident irradiance during the period. In Lake 5, NEP rates were close to zero until late May after which low positive daily rates were common. In contrast, NEP rates in Lake 4 were predominantly positive during the entire studied

Table 2 Volumetric and areal rates of GPP, R and NEP in the five investigated lakes

Lake	Site	Year	Lake days (n)	GPP ($g\ O_2\ m^{-3}\ day^{-1}$)	R	NEP	GPP ($g\ O_2\ m^{-2}\ day^{-1}$)	R	NEP
1		2015	4	49.8 (42.4–63.4)	41.8 (32–63.2)	8 (0.2–16.2)	11 (9.3–14)	9.2 (7–13.9)	1.8 (0.1–3.6)
3			4	24.6 (18.9–33.2)	33.8 (26.5–41.2)	−9.2 (−15.6–3.7)	1.2 (0.9–1.7)	1.7 (1.3–2.1)	−0.5 (−0.8–0.2)
4	A		63	14.1 (1.7–36.7)	12.3 (1.8–34.6)	1.7 (−1.8–10.3)	3.3 (0.4–7.4)	2.9 (0.5–7.3)	0.4 (−0.4–2)
	B		63	13 (2.3–36.7)	11.7 (2.4–35.5)	1.2 (−1.4–7.1)	3.0 (0.6–7.9)	2.7 (0.6–7.6)	0.3 (−0.4–1.5)
	C		63	16.6 (3.2–64.5)	9.8 (2.4–37.5)	6.8 (−0.5–44.4)	3.8 (0.8–12.5)	2.3 (0.6–7.1)	1.5 (−0.1–8.6)
	D		18	35.3 (12.6–61.2)	33.7 (6.5–60.1)	1.6 (−1.4–8.5)	7.7 (2.7–12.2)	7.4 (1.4–12)	0.3 (−0.4–1.7)
5	A		63	13.2 (2.4–29.5)	12.7 (2.6–28)	0.5 (−1.0–4.4)	2.2 (0.4–4.9)	2.2 (0.5–4.6)	0.1 (−0.2–0.7)
	B		4	42 (24.6–62.9)	43.2 (24.3–63.6)	−1.2 (−4.0–0.4)	6.7 (3.9–10.1)	6.9 (3.9–10.2)	−0.2 (−0.6–0.1)
1		2016	9	46.5 (38.4–52.4)	38.9 (31.4–47.5)	7.6 (2.2–17.3)	14.2 (11.8–16.4)	11.8 (8.7–14.6)	2.3 (0.6–4.8)
2			9	73.8 (50.3–92.3)	64.6 (39.4–89.8)	9.2 (−1.1–18.8)	12.4 (9.9–15.3)	10.9 (7.7–14.9)	1.5 (−0.2–2.6)
3			9	29.5 (17.7–41.5)	29.0 (16.5–41.8)	0.5 (−2.1–1.6)	3.4 (2.0-4.8)	3.3 (1.9–4.8)	0.1 (−0.2–0.2)
4	A		10	28.4 (20.3–36.6)	22.4 (12.7–30.8)	6.0 (2.1–13.0)	8.9 (6.0–12.0)	7.1 (3.5–10.2)	1.8 (0.6–3.6)

Mean values with ranges in parenthesis

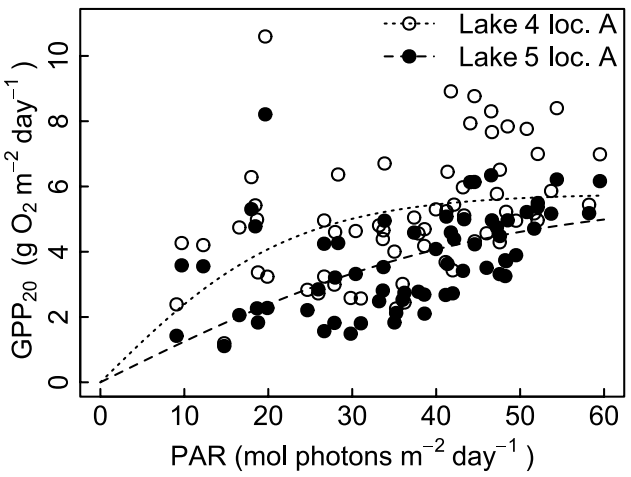

Fig. 4 GPP_{20} areal rates ($g\ O_2\ m^{-2}\ day^{-1}$) as a function of incident irradiance (PAR, mol $m^{-2}\ day^{-1}$) in Lakes 4 (*open circles*) and 5 (*closed circles*). The *curves* are fitted by a hyperbolic relationship (Eq. 3)

period (Fig. 3; Table 2). The Jassby-Platt model (Eq. 3) fitted to daily GPP rates and normalized to 20 °C showed a positive relationship to daily incident irradiance with a tendency towards saturation on days of high irradiance (Fig. 4).

The charophyte dominated lakes obtained high metabolic rates during early summer. Metabolic rates were highest in Lake 1 and 2, slightly lower in Lake 4 and 5 and lowest in Lake 3 (Figs. 3, 5). Compared to deeper and larger lakes (Hanson et al. 2003; Solomon et al. 2013), volumetric rates of GPP and R were very high (Table 2; Fig. 6). Despite the shallow water in the charophyte lakes, areal rates were also relatively high compared to other types of aquatic ecosystems (Fig. 7). The high volumetric rates gave rise to extreme diel fluctuations in surface water oxygen saturation. This variability was particularly pronounced in Lake 2 (mean 120% saturation; range 6–279%), where low nighttime oxygen minima (mean 19% saturation, range 6–59%) were frequent during summer 2016.

The balance between GPP and R (NEP) was predominantly positive during spring and summer in all charophyte lakes in both years, except for very shallow sites (<0.1 m in Lake 3 and Lake 5 loc. B), which mostly exhibited negative NEP rates during summer 2015 (Table 2). Positive NEP rates are in agreement with the average oxygen supersaturation measured in surface waters of the studied lakes. During summer 2016, NEP was positive in all lakes and of the same level in Lake 1, 2 and 4. However, NEP in Lake 3 was close to zero (Table 2; Fig. 5).

Day-to-day variation

During spring 2015, day-to-day variations of GPP and R were low in Lake 4 and 5 (Fig. 3). Changes were gradual and sudden day-to-day changes were rare and small. Day-to-day variations were more common for R than for GPP. In the different locations in Lake 4, significant day-to-day differences in metabolism (characterized by non-overlapping 95% CI) occurred on 22–25% occasions for R and only 3–12% occasions for GPP. In Lake 5 loc. A, the significant day-to-day variability was 27% for R and 8% for GPP. During summer 2016, significant day-to-day differences were very rare; of all occasions, only 4% for R and 11% for GPP (Fig. 5).

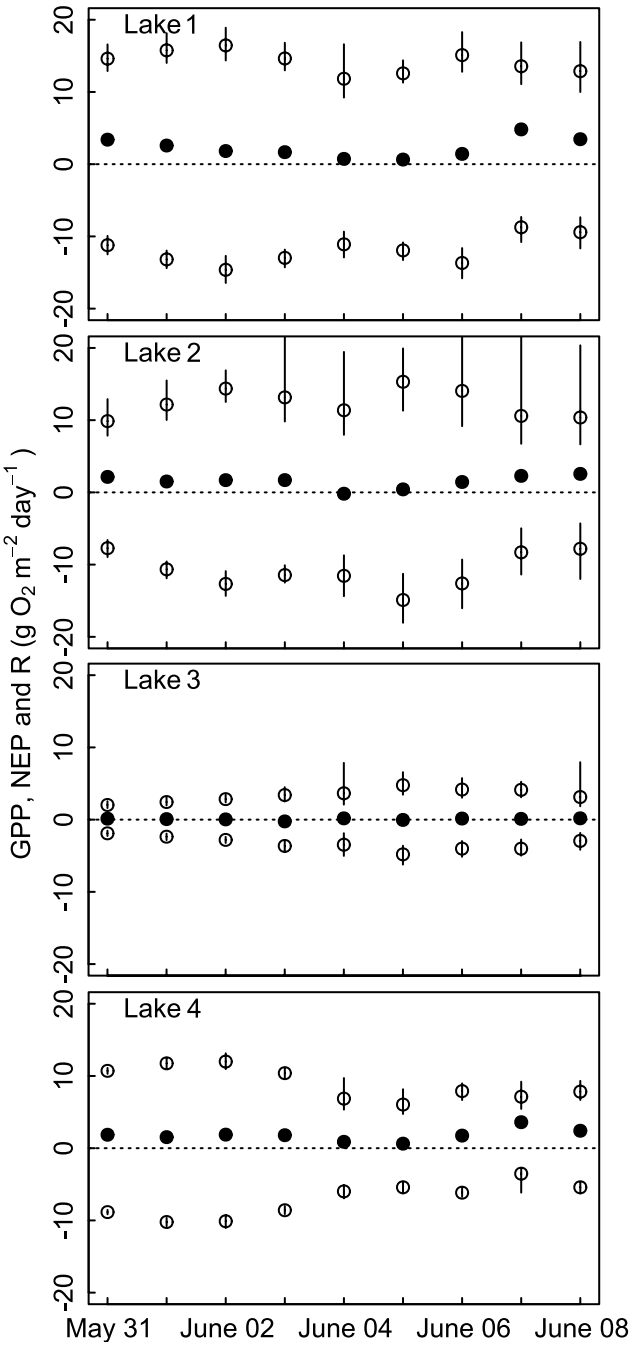

Fig. 5 Areal metabolic rates (g O_2 m^{-2} day^{-1}) in four charophyte lakes studied in summer 2016. Daily GPP and R rates (*open circles*) with 95% CI and NEP (*filled circles*) are shown

Respiration-production coupling and baseline respiration

During spring 2015, daily values of GPP and R were closely coupled in Lake 4 loc. A–C and Lake 5 loc. A. Slopes for R (y) vs. GPP (x) ranged from 0.88 to 0.93 for most locations with deeper water and high charophyte biomass to only 0.62 for the shallow location with low charophyte cover (Fig. 6, S2). While the slope differed, the 95% CI of the intercepts (R_{base}) were not significantly different from zero in Lake 4 loc. A–C, which implies that background respiration was negligible. Despite being significantly positive, background respiration was very low in Lake 5 loc. A. Analysis of all four lakes during 9–10 days in June 2016 confirmed the close coupling between R and GPP with a common slope of 0.90 and a low intercept (−1.48 g O_2 m^{-3} day^{-1}), which was not significantly different from zero (Fig. 6). This finding is in agreement with the analysis for individual lakes. Thus, in these shallow charophyte lakes, respiration is closely coupled to lake production on the same day and background respiration is low or negligible.

Discussion

Submerged macrophytes and temperature gradients

The present analysis confirmed that small, shallow lakes with dense macrophyte vegetation undergo extreme diel temperature cycles (Andersen et al. 2016). Large diel variations in surface water temperatures at about 15 °C are possible due to a shallow mixed surface layer and high light attenuation. The observed high diel temperature range is not uncommon among small lakes (Woolway et al. 2016). Steep vertical stratification also developed during the day as a result of high light absorption in the dense charophyte canopy, while cooling of surface waters during the evening and night induced convective mixing (Andersen et al. 2016). Although it has previously been shown that submerged macrophyte stands can induce large temperature gradients (Dale and Gillespie 1977), the magnitude of temperature gradients demonstrated here for such shallow water columns is much greater than anticipated and unprecedented in previous studies. Because of the high submerged macrophyte biomass, the stratification-mixing cycle is a recurring daily phenomenon. Only modest surface heating is required for daytime stratification to develop as wind induced turbulence is rapidly dissipated by the charophyte canopy (Andersen et al. 2016). Daytime stratification was only absent on very cold, windy or rainy days during spring–summer.

Modeling ecosystem metabolism

A consequence of diel stratification is that the oxygen signal recorded from surface waters only reflects processes in the mixed surface layer during the day, but the entire water column at night. This should not affect our estimate of GPP because light only penetrates few centimeters into the

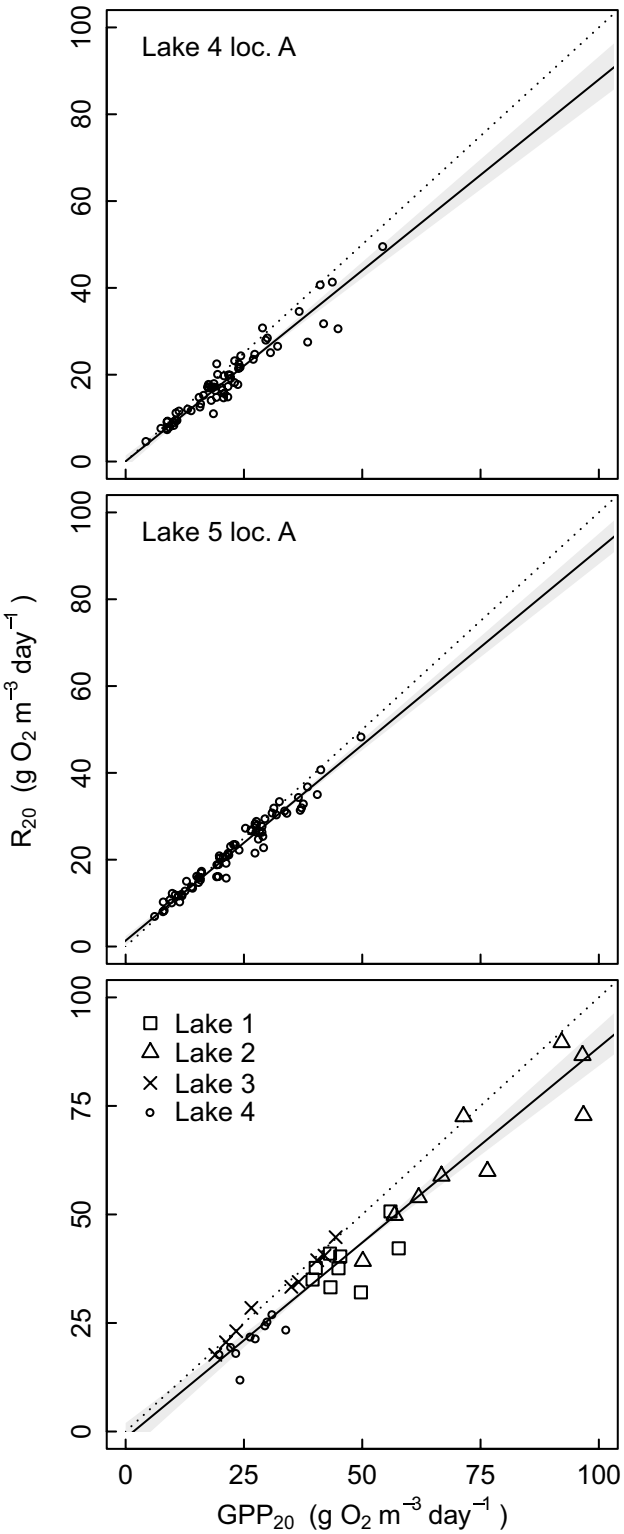

Fig. 6 Linear relationship of daily rates of R (g O_2 m^{-3} day^{-1}) versus GPP (g O_2 m^{-3} day^{-1}) in Lakes 4, 5 (2015) along with the four lakes studied during 2016 (*solid line*, standard major axis regression). Shown are 95% CI (*grey area*) and the 1:1 linear relationship (*dotted line*). Rates are per unit volume and normalized to 20 °C. Regression parameter estimates of intercept (R_{base}) and slope (β) with 95% CI in parenthesis are: Lake 4 loc. A: $R_{base}=0.05$ (−1.4–1.4) and $\beta=0.88$ (0.82–0.95), Lake 5 loc. A: $R_{base}=1.36$ (0.29–2.39) and $\beta=0.90$ (0.86–0.95) and Lakes 1, 2, 3 and 4 (2016): $R_{base}=-1.48$ (−5.25–1.96) and $\beta=0.90$ (0.82–0.98)

charophyte canopy owing to high light attenuation, which is also the main driver of thermocline development. Oxygen produced by photosynthesis is released to the mixed surface layer, and production below the thermocline is negligible. Respiration is estimated at night when photosynthesis is zero and the water column is well mixed and thus should encompass all ecosystem components, seeing that the nocturnal convective mixing is quite efficient (Andersen et al. 2016). Overestimation of NEP could occur when respiratory processes in bottom waters do not influence the oxygen signal recorded in surface waters during stratification. In Lake 4 during 2016, water volume below the thermocline constituted only 8–14% of the total volume. Therefore, estimates of lake metabolism by the described procedure include the relevant major components and processes. This conclusion is supported by the close agreement between observed and modeled diel oxygen signals, with generally narrow 95% CI's.

The observed oxygen signal in surface waters was well predicted by using the applied model (Eqs. 2–7). On most days, uncertainty of metabolism estimates was well constrained by the bootstrap analysis. Variation between observed and modeled oxygen signals may arise from processes not included in the model (Eq. 2), such as advective mixing or respiratory substrate limitation (McNair et al. 2013). Modeling the gas transfer velocity as a function of wind may also introduce error due to the fact that near-surface turbulence in small lakes is influenced by convective mixing (Read et al. 2012). Convective mixing is driven by heat loss from surface waters and, with the high diel temperature range observed in the investigated lakes, convective mixing could contribute to near-surface turbulence (Holgerson et al. 2016; MacIntyre et al. 2010). However, the applied empirical model was the best available for use in small lakes within the size range investigated here; it was derived from previous measurements in Lake 4 (Andersen 2015).

High rates of ecosystem metabolism

The summer metabolic rates reported here are probably close to annual maximum rates because temperature and irradiance were both high. Volumetric metabolic rates estimated in this study are very high compared to values from other aquatic systems (Duarte and Agustí 1998; Solomon et al. 2013). The high volumetric metabolic rates are attributed to the high charophyte biomass, shallow photic zone and high light availability in the upper canopy.

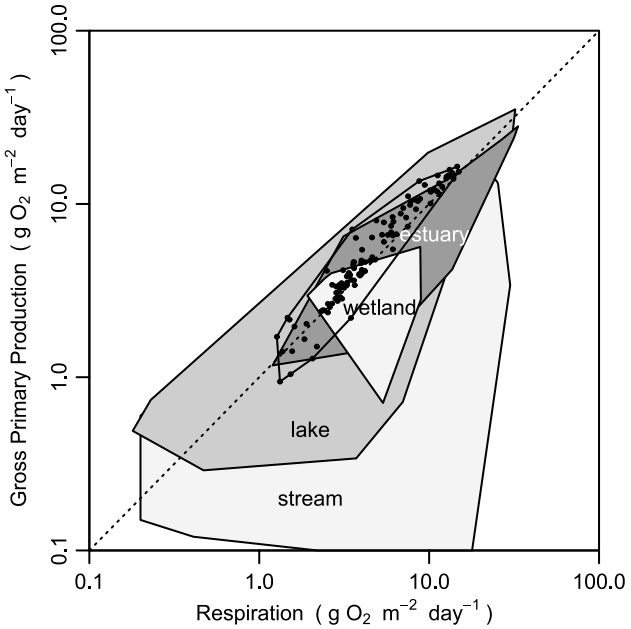

Fig. 7 Aquatic ecosystem metabolism showing GPP versus R during summer for a data compilation from different aquatic ecosystems (Hoellein et al. 2013). *Filled circles* are daily rates of metabolism from measurements on shallow charophyte lakes during May and June in the present study (n = 111). The data ranges in the different ecosystems are enclosed within the covered areas

Metabolic rates normalized to area are also high compared to other aquatic ecosystems (Fig. 7), because of the high proportion of incident irradiance absorbed by photosynthetic pigments. Absorption in these clear lakes not owing to photosynthetic pigments is likely to stem from precipitated $CaCO_3$ as well as associated colored components on the surfaces of charophytes.

The high volumetric rates of production result in high demands for dissolved inorganic carbon (DIC) in surface waters. The charophyte lakes are located on calcareous rock and have average DIC concentrations of 0.7–2.7 mM mainly available for photosynthesis in the form of bicarbonate (HCO_3^-). Free CO_2 has been shown to be used five to six times more readily than HCO_3^- by the dominant charophyte species (*Chara aspera*) in the lakes (Van den Berg et al. 2002), which requires active ion-transport (Lucas and Berry 1985). Bicarbonate is present typically in 10- to 100-fold higher concentrations in the charophyte lakes, and is the most important and stable source of inorganic carbon to charophyte photosynthesis (Madsen and Sand-Jensen 1991). The continuously high GPP rates in the charophyte lakes are unlike those of deep lakes with seasonal stratification in which gradual epilimnetic depletion of nutrients and DIC increasingly limits primary production during summer (Brighenti et al. 2015; Staehr and Sand-Jensen 2007). In the charophyte lakes, photosynthesis can be constrained by reduced DIC in the afternoon (Andersen 2015), but the DIC pool is re-established by nocturnal mixing because $CaCO_3$ is dissolved and organic matter is degraded in the bottom waters during the stratification period. Thus, regeneration of DIC and nutrients, mixing and reinjection of resources into surface waters are daily recurring phenomena, which can sustain high GPP rates.

During the summer 2016, volumetric rates of GPP and R in Lake 2 averaged at 74 (range 50–92) and 65 (range 39–90) g O_2 m^{-3} day^{-1}, respectively (Table 2). These values correspond to oxygen pool turnover times of only 3.4–3.8 h. Despite a shorter turnover time of the oxygen pool than the duration of the night (5.5–6 h summer 2016), Lake 2 did not turn anoxic, though nocturnal oxygen minima were low. The lack of anoxia was probably due to enhanced gas exchange as surface water oxygen decreased and respiratory substrate limitation as previously demonstrated by large nocturnal decline of ecosystem respiration in free-water measurements in Lake 4, and confirmed by charophyte respiration in bottle incubations (Andersen 2015).

Net ecosystem production

Positive NEP values imply that ecosystems are net autotrophic and have a production surplus which can be incorporated into additional charophyte biomass, or accumulated in the sediment as organic matter (Staehr et al. 2012). Solomon et al. (2013) found that mean summer NEP values in 25 globally distributed lakes ranged between −7.3 and 9.9 g O_2 m^{-2} day^{-1} [−7.0 and 1.5 for lakes with total-P < 20 L^{-1}, Hoellein et al. (2013)]. The charophyte lakes studied here have oligotrophic waters and most nutrients are incorporated into charophyte biomass and buried in the sediments (Christensen et al. 2013). From this analysis, it cannot be concluded whether these charophyte lakes are net autotrophic or net heterotrophic on an annual scale, but they are probably close to zero or slightly net autotrophic as shown previously for Lake 4 (Christensen et al. 2013). Only thin sediments have built up in the deeper parts during the lakes' 30 years of existence, and it shows that storage of organic carbon and dead charophyte fragments within the systems are low. Allochthonous organic carbon would contribute to this storage, but is low due to the sparse terrestrial vegetation and the restricted water input.

An earlier study of a charophyte lake on Räpplinge alvar also found that NEP was slightly positive during spring and early summer (0.2–1.4 g O_2 m^{-2} day^{-1}), but negative during desiccation in mid-summer and positive again in August in the time of refilling (Christensen et al. 2013). For the period studied here, the water depth did not reach the critical threshold in the deeper charophyte lakes. NEP ranged between −0.8 and 4.8 g O_2 m^{-2} day^{-1}, but was

predominantly positive. However, as a result of desiccation, periods of negative NEP were observed in the shallow Lake 3 and the shallow location Lake 5 loc. B during summer 2015.

Measurements show that sediment respiration is low in the charophyte lakes (Andersen 2015). The positive NEP is mainly utilized by the charophytes for growth. Converting previously measured sediment respiration from Lake 4 (Andersen 2015) at 15 °C to diel mean temperature, applying a Q_{10} value of 2.0 for the summer 2016, revealed that sediment respiration (R_{sed}) constituted, on average, 12% of total ecosystem respiration during the period in Lake 4 (Fig. 5). Respiration in free water is negligible and the main driver of both GPP and R is the large charophyte biomass (Andersen 2015). Assuming that respiration is only a result of charophytes (R_{Chara}) and sediments (R_{sed}), the net charophyte production (NP_{Chara}) can be estimated as $NP_{Chara} = NEP + R_{sed}$. For the 2016 summer period, this yields mean NEP values of 1.8 and NP_{Chara} of 2.6 g O_2 m^{-2} day^{-1}. This surplus is at the same level as the possible daily increase of charophyte biomass in g organic dry matter m^{-2}, which is equivalent to a biomass accumulation of about 200–300 g organic dry matter m^{-2} over 4 months in agreement with the measured level of charophyte biomass. Similar levels were reported by Christensen et al. (2013).

R-GPP coupling and baseline respiration

By applying regression analysis, a close coupling of R and GPP daily estimates was found. This finding was supported by data from Lake 4 and 5 in spring 2015 as well as Lake 1, 2, 3 and 4 in summer 2016. The very low or zero background respiration implies that terrestrial contribution to ecosystem metabolism is low or negligible during the spring–summer periods in the five charophyte lakes. The pool of more recalcitrant organic matter would likely consist of particulate matter from the sparse terrestrial vegetation, but otherwise be dominated by detritus from dead charophytes. Tight R-GPP coupling has previously been shown in nutrient-poor lakes (Richardson et al. 2016; Sadro et al. 2011; Solomon et al. 2013), as well as in Spanish shallow lakes with high metabolic rates (Geertz-Hansen et al. 2011).

As a result of the small lake sizes, low horizontal heterogeneity of metabolism estimates was expected. Previous studies in larger lakes have found substantial spatial variation of metabolism within lakes (Lauster et al. 2006; Van de Bogert et al. 2012), which suggests that the mixed surface layer is not necessarily well mixed horizontally, or that the rates of turbulence are low compared to the local differences of metabolism. The shallow location C in Lake 4 is different from location A, B and D by being susceptible to desiccation resulting in a less dense and shorter charophyte canopy. This difference could explain the high GPP relative to R at this location. When self-shading is low in the canopy it will require less respiration in order to sustain the lower biomass.

Comparison of ecosystem metabolism across aquatic systems

A recent comprehensive study compiled estimates of ecosystem metabolism in different aquatic systems (Hoellein et al. 2013), for which we have added metabolic rates from the present study of shallow vegetated lakes (Fig. 7). The small oligotrophic vegetated lakes studied here do not fit the expectation that GPP should increase along a gradient of total P concentration as observed in larger lakes (Hanson et al. 2008; Solomon et al. 2013). The very low phosphate levels measured in Lake 3 and 4 are likely characteristic for all the investigated lakes located within short distances on the nutrient-poor alvar. The pattern can be explained by the dominance of benthic primary producers in the small lakes in contrast to the dominance of pelagic production by phytoplankton in larger, deeper lakes (Kalff 2002).

Daily GPP is positively related to daily incident light utilized by a high density of photosynthetic pigments. The biomass of phytoplankton communities is often nutrient limited and is much higher in eutrophic than oligotrophic lakes (Kalff 2002). Maximum rates of photosynthesis relative to absorbed light are, however, comparable for phytoplankton- and submerged macrophyte communities (Krause-Jensen and Sand-Jensen 1998). As a result, the same high areal rates of GPP can be reached in dense charophyte stands in shallow, oligotrophic lakes as in deeper phytoplankton-rich water columns of eutrophic lakes (Krause-Jensen and Sand-Jensen 1998).

Previous studies have shown that small lakes are active sites of carbon processing and atmospheric carbon emission compared to medium-sized and large lakes (Holgerson and Raymond 2016; Sand-Jensen and Staehr 2007). Their role in global carbon budgets is open to debate because of the uncertainties associated with the estimation of the number and surface area of small lakes (Downing et al. 2006; Verpoorter et al. 2014). Using the areas for small lakes (<0.01 km^2) and larger lakes (>0.01 km^2) reported by Downing et al. (2006), and the median areal GPP and R reported in this study and the lakes compiled in Hoellein et al. (2013), show that 30 and 21% of the global lake GPP and R may take place in small lakes. The values of GPP in the small, shallow lakes dominated by submerged macrophytes are probably higher than for many small lakes devoid of macrophytes. Nonetheless, the evaluation supports the notion that small aquatic systems are very important components of global carbon processing.

Acknowledgements This work was supported by grants to KSJ from the Carlsberg Foundation to the study of small lakes and Center of Excellence to Lake Restoration from the Villum Kann Rasmussen Foundation. We thank Sara Schousboe for linguistic corrections.

References

Alnoee AB, Riis T, Andersen MR, Baattrup-Pedersen A, Sand-Jensen K (2015) Whole-stream metabolism in nutrient-poor calcareous streams on Öland, Sweden. Aquat Sci 77:207–219. doi:10.1007/s00027-014-0380-5

Andersen MR (2015) Ecology in small aquatic ecosystems. Ph.D. thesis, University of Copenhagen

Andersen MR, Sand-Jensen K, Iestyn Woolway R, Jones ID (2016) Profound daily vertical stratification and mixing in a small, shallow, wind-exposed lake with submerged macrophytes Aquat Sci. doi:10.1007/s00027-016-0505-0

Binzer T, Sand-Jensen K, Middelboe A-L (2006) Community photosynthesis of aquatic macrophytes. Limnol Oceanogr 51:2722–2733. doi:10.4319/lo.2006.51.6.2722

Brighenti LS et al (2015) Seasonal changes in metabolic rates of two tropical lakes in the Atlantic forest of Brazil. Ecosystems 18:589–604. doi:10.1007/s10021-015-9851-3

Christensen J, Sand-Jensen K, Staehr PA (2013) Fluctuating water levels control water chemistry and metabolism of a charophyte-dominated pond. Freshw Biol 58:1353–1365. doi:10.1111/fwb.12132

Dale HM, Gillespie TJ (1977) Influence of submersed aquatic plants on temperature-gradients in shallow-water bodies. Can J Bot 55:2216–2225. doi:10.1139/b77-251

Del Giorgio PA, Cole JJ, Caraco NF, Peters RH (1999) Linking planktonic biomass and metabolism to net gas fluxes in northern temperate lakes. Ecology 80:1422–1431. doi:10.2307/177085

Downing JA (2010) Emerging global role of small lakes and ponds: little things mean a lot. Limnetica 29:9–24

Downing J et al (2006) The global abundance and size distribution of lakes, ponds, and impoundments. Limnol Oceanogr 51:2388–2397. doi:10.4319/lo.2006.51.5.2388

Duarte CM, Agustí S (1998) The CO_2 balance of unproductive aquatic ecosystems. Science 281:234–236. doi:10.1126/science.281.5374.234

Efron B, Tibshirani RJ (1993) An introduction to the bootstrap. Monographs on statistics and applied probability, vol 57. Chapman & Hall, New York

Geertz-Hansen O, Montes C, Duarte CM, Sand-Jensen K, Marbà N, Grillas P (2011) Ecosystem metabolism in a temporary Mediterranean marsh (Doñana National Park, SW Spain). Biogeosciences 7:6495–6521. doi:10.5194/bgd-7-6495-2010

Gran G (1952) Determination of the equivalence point in potentiometric titrations. Part II. Analyst 77:661–671. doi:10.1039/an9527700661

Hanson PC, Bade DL, Carpenter SR, Kratz TK (2003) Lake metabolism: relationships with dissolved organic carbon and phosphorus. Limnol Oceanogr 48:1112–1119. doi:10.4319/lo.2003.48.3.1112

Hanson PC, Carpenter SR, Kimura N, Wu C, Cornelius SP, Kratz TK (2008) Evaluation of metabolism models for free-water dissolved oxygen methods in lakes. Limnol Oceanogr Methods 6:454–465. doi:10.4319/lom.2008.6.454

Hilborn R, Mangel M (1997) The ecological detective: confronting models with data. Monographs in population biology, vol 28. Princeton University Press, New Jersey

Hoellein TJ, Bruesewitz DA, Richardson DC (2013) Revisiting Odum (1956): a synthesis of aquatic ecosystem metabolism. Limnol Oceanogr 58:2089–2100. doi:10.4319/lo.2013.58.6.2089

Holgerson MA, Raymond PA (2016) Large contribution to inland water CO_2 and CH_4 emissions from very small ponds. Nature Geosci 9:222–226. doi:10.1038/ngeo2654

Holgerson MA, Zappa CJ, Raymond PA (2016) Substantial overnight reaeration by convective cooling discovered in pond ecosystems. Geophys Res Lett 43:8044–8051. doi:10.1002/2016gl070206

Jähne B, Heinz G, Dietrich W (1987) Measurement of the diffusion coefficients of sparingly soluble gases in water. J Geophys Res 92:10767–10776. doi:10.1029/jc092ic10p10767

Jassby AD, Platt T (1976) Mathematical formulation of the relationship between photosynthesis and light for phytoplankton. Limnol Oceanogr 21:540–547. doi:10.4319/lo.1976.21.4.0540

Jørgensen SE, Bendoricchio G (2001) Fundamentals of ecological modelling vol 21. Developments in environmental modelling. Elsevier, Amsterdam

Kalff J (2002) Limnology: inland water ecosystems. Prentice Hall, New Jersey

Kragh T, Andersen MR, Sand-Jensen K (2017) Profound afternoon depression of ecosystem production and nighttime decline of respiration in a macrophyte-rich shallow lake. Oecologia **(in press)**

Krause-Jensen D, Sand-Jensen K (1998) Light attenuation and photosynthesis of aquatic plant communities. Limnol Oceanogr 43:396–407. doi:10.4319/lo.1998.43.3.0396

Lauster GH, Hanson PC, Kratz TK (2006) Gross primary production and respiration differences among littoral and pelagic habitats in northern Wisconsin lakes. Can J Fish Aquat Sci 63:1130–1141. doi:10.1139/f06-018

Lewis E, Wallace D (1998) Program Developed for CO_2 System Calculations (Carbon Dioxide Information Analysis Center, Oak Ridge National Laboratory, US Department of Energy, Oak Ridge, TN) ORNL/CDIAC-105

Lucas WJ, Berry JA (1985) Inorganic carbon transport in aquatic photosynthetic organisms. Physiol Plant 65:539–543. doi:10.1111/j.1399-3054.1985.tb08687.x

MacIntyre S, Jonsson A, Jansson M, Aberg J, Turney DE, Miller SD (2010) Buoyancy flux, turbulence, and the gas transfer coefficient in a stratified lake Geophys Res Lett. doi:10.1029/2010gl044164

Madsen TV, Sand-Jensen K (1991) Photosynthetic carbon assimilation in aquatic macrophytes. Aquat Bot 41:5–40. doi:10.1016/0304-3770(91)90037-6

McNair JN, Gereaux LC, Weinke AD, Sesselmann MR, Kendall ST, Biddanda BA (2013) New methods for estimating components of lake metabolism based on free-water dissolved-oxygen dynamics. Ecol Model 263:251–263. doi:10.1016/j.ecolmodel.2013.05.010

Odum HT (1956) Primary production in flowing waters. Limnol Oceanogr 1:102–117. doi:10.4319/lo.1956.1.2.0102

Politis DN (2003) The impact of bootstrap methods on time series analysis. Stat Sci 18:219–230. doi:10.1214/ss/1063994977

R Core Team (2016) R: a language and environment for statistical computing. R Foundation for Statistical Computing, Vienna

Read JS et al (2011) Derivation of lake mixing and stratification indices from high-resolution lake buoy data. Environ Model Softw 26:1325–1336 doi:10.1016/j.envsoft.2011.05.006

Read JS et al (2012) Lake-size dependency of wind shear and convection as controls on gas exchange Geophys Res Lett. doi:10.1029/2012gl051886

Richardson DC, Carey CC, Bruesewitz DA, Weathers KC (2016) Intra-and inter-annual variability in metabolism in an oligotrophic lake Aquat Sci. doi:10.1007/s00027-016-0499-7

Sadro S, Melack JM, MacIntyre S (2011) Spatial and temporal variability in the ecosystem metabolism of a high-elevation lake:

integrating benthic and pelagic habitats. Ecosystems 14:1123–1140. doi:10.1007/s10021-011-9471-5

Sand-Jensen K, Staehr PA (2007) Scaling of pelagic metabolism to size, trophy and forest cover in small Danish lakes. Ecosystems 10:128–142. doi:10.1007/s10021-006-9001-z

Sand-Jensen K, Båstrup-Spohr L, Andersen MR, Christensen JPA, Alnoee AB, Jespersen TS (2015) Mellan torka och översvämning på Öland Sven Bot Tidskr 109:28–35

SMHI Swedish Meteorological and Hydrological Institute. http://www.smhi.se/klimatdata. Accessed June 2016

Solomon CT et al (2013) Ecosystem respiration: drivers of daily variability and background respiration in lakes around the globe. Limnol Oceanogr 58:849–866. doi:10.4319/lo.2013.58.3.0849

Staehr PA, Sand-Jensen K (2007) Temporal dynamics and regulation of lake metabolism. Limnol Oceanogr 52:108–120. doi:10.4319/lo.2007.52.1.0108

Staehr PA, Testa JM, Kemp WM, Cole JJ, Sand-Jensen K, Smith SV (2012) The metabolism of aquatic ecosystems: history, applications, and future challenges. Aquat Sci 74:15–29. doi:10.1007/s00027-011-0199-2

Van de Bogert MC, Carpenter SR, Cole JJ, Pace ML (2007) Assessing pelagic and benthic metabolism using free water measurements. Limnol Oceanogr Methods 5:145–155. doi:10.4319/lom.2007.5.145

Van de Bogert MC, Bade DL, Carpenter SR, Cole JJ, Pace ML, Hanson PC, Langman OC (2012) Spatial heterogeneity strongly affects estimates of ecosystem metabolism in two north temperate lakes. Limnol Oceanogr 57:1689–1700. doi:10.4319/lo.2012.57.6.1689

Van den Berg MS, Coops H, Simons J, Pilon J (2002) A comparative study of the use of inorganic carbon resources by *Chara aspera* and *Potamogeton pectinatus*. Aquat Bot 72:219–233. doi:10.1016/s0304-3770(01)00202-9

Vermeer CP, Escher M, Portielje R, de Klein JJM (2003) Nitrogen uptake and translocation by Chara. Aquat Bot 76:245–258. doi:10.1016/s0304-3770(03)00056-1

Verpoorter C, Kutser T, Seekell DA, Tranvik LJ (2014) A global inventory of lakes based on high-resolution satellite imagery. Geophys Res Lett 41:6396–6402. doi:10.1002/2014gl060641

Wanninkhof R (1992) Relationship between wind speed and gas exchange over the ocean. J Geophys Res Oceans 97:7373–7382. doi:10.1029/92jc00188

Weiss RF (1970) The solubility of nitrogen, oxygen and argon in water and seawater. Deep Sea Res Oceanogr Abstr 17:721–735. doi:10.1016/0011-7471(70)90037-9

Woolway RI et al (2016) Diel surface temperature range scales with lake size. PLoS One 11:e0152466. doi:10.1111/j.1365-2656.2010.01731.x